ЯДЕРНА ФІЗИКА
NUCLEAR PHYSICS

УДК 539.17.02:539.172:615.849

https://doi.org/10.15407/jnpae2021.03.237

Glara Fuad Hasan[1,2,3,*], Edrees Muhammad-Tahir Nury[1], Flavia Groppi[2,3]

[1] *Department of Physics, College of Education, University of Salahaddin, Erbil, Iraq*
[2] *Department of Physics, University of Milan, Milan, Italy*
[3] *Accelerator and Superconductivity Laboratory* (*LASA*),
Department of Physics, University of Milan and the National Institute of Nuclear Physics (*INFN*),
Segrate (*MI*), *Italy*

*Corresponding author: gelara.hassan@su.edu.krd

EVALUATION OF CROSS-SECTION DATA FOR RADIONUCLIDES USED IN POSITRON EMISSION TOMOGRAPHY BY EFFECTS OF LEVEL DENSITY MODELS USING EMPIRE 3.2.2 CODE

This work presents the evaluated results of cross-sections for natural chromium (^{nat}Cr) with several nuclear reactions of ^{nat}Cr(d, x)$^{52g,\,m+}$Mn, ^{nat}Cr(d, x)^{54}Mn, ^{nat}Cr(d, x)^{51}Cr, and ^{nat}Cr(d, x)^{48}V using the statistical nuclear model EMPIRE 3.2.2 code with different level density models, for some radionuclides used in positron emission tomography. We compared the results to data sets found in literature, and data chosen from various sets of the electronic TENDL library.

Keywords: Mn radioisotopes, positron emission tomography scan, cross-section, nuclear medicine, EMPIRE 3.2.2 code.

1. Introduction

The use of radioisotopes in nuclear medical imaging has grown through revolution and evolution, largely attributable to the development of a new nuclear imaging technology [1]. The positron emission tomography (PET) is defined as a nuclear medical imaging technique with the specificity and sensitivity necessary for imaging molecular pathways in a non-invasive, and in vivo manner [2, 3]. Given the growing interest in therapeutic and nuclear medicine imaging, the demand for more and different radionuclides has increased. Importantly, types of radionuclides play significant roles in new technological applications for use in daily life, as well as in scientific research [4 - 6]. The ^{52}Mn radionuclide has paramagnetic parameters and is potentially important in image development as a contrast agent for manganese-enhance magnetic resonance imaging (MEMRI) and magnetic resonance imaging (MRI). In addition, ^{52g}Mn can be used for dual PET/MRI. The best manganese to use in this case has a suitable half-life, such as ^{52}Mn (5.591 days), ^{52m}Mn (21.1 min), particularly for use as a PET tracer in PET imaging [7]. To optimize the production routes, the deuteron induced cross-section is desired, for the optimization of the radioisotope produced, full knowledge of the input parameter EMPIRE code to obtain cross-sections data can be used to test the various nuclear level density of the nuclear reaction. For some of the radioisotopes that were used to get the PET image, the deuteron cross-section induced by nuclear reactions was calculated aided an EMPIRE 3.2.2 code, the most updated version of the simulation series [8]. Therefore, these deuteron-induced cross-section data sets obtained from theoretical models play an important role in the study of deuteron-induced nuclear reactions and they can be used by evaluators to interpolation and extrapolation.

The evaluation of cross-sections for the deuteron energy up to 35 MeV has been done by using the EMPIRE 3.2.2 code contributing various density level models for the excitation functions of $^{52g,m+}$Mn, ^{54}Mn, ^{51}Cr, and ^{48}V. The obtained results were compared and analyzed with literature data as well as TENDL electronic library.

2. EMPIRE model calculations

Cross-section determination plays an important role in the development of the calculations of nuclear reaction models. This work is focused on the calculations that were carried out with the nuclear reaction simulation EMPIRE code. The EMPIRE 3.2.2 code (theoretical computer code of nuclear reactions) approach was developed by Herman et al. and is useful to estimate the evaluated nuclear cross-section data sets of various particles and a broad range of energies. In this computer code, each of the input parameters has a significant role in the results. An input parameter is based on the Reference Input Parameter Library or RIPL-3, a library covering nuclear masses, discrete levels, optical models, decay schemes, and the levels of densities parameters. The optical model parameters in the calculations were

obtained from RIPL-3, the optical model potential (OMP) of deuteron energy used was proposed by Haixia An and Chonghai Cai [9]. Since the OMP was selected for use in this study, the densities of the nuclear levels were provided by means of different parameters. The statistical calculation of various nuclear-level density parameters was employed to estimate the cross-sections. Considering this, we can see the different results of different level density models factor for other medical radioisotopes [10 - 15]. In EMPIRE 3.2.2 the results of the cross-section substantially depend on the parameters of the level density. Each model of nuclear level density is related to different parameterizations concerning considerations of deformation and the excitation energy and collective phenomena of the target nuclei. This present simulation included the following level density models.

LEVDEN = 0 is the EMPIRE enhanced generalized superfluid model (EGSM), designed to (RIPL-3) to separate the levels and experimental value of D_{obs}. This is a default model used in EMPIRE code.

LEVDEN = 1 is the EMPIRE generalized superfluid model (GSM), designed to RIPL to separate the levels and experimental value of D_{obs}.

LEVDEN = 2 is the EMPIRE Gilbert - Cameron model (GCM), designed to RIPL to separate the levels and experimental value of D_{obs} (it stimulates separating the excitation energy into two different parts; in each of the regions, different forms functional of level densities are used).

LEVDEN = 3 is the RIPL-3 microscopic Hartree - Fock - Bogoliubov model (HFBM), D_{obs} is the neutron resonance spacing [16].

The obtained results by default LEVDEN = 0 in EMPIRE 3.2.2 code for all four reactions were not in accord with our experimental data sets up to 35 MeV [17], in this case for to have a suitable curve for the calculated simulation achievement results and the available experimental data sets, to adjust the value of the default level density in EGSM [18], in adjusting the asymptotic value of a-parameter, that is equivalent to fix the parameter of level density, to obtain good results for each reaction and comparison with the experimental data, both the ATILNO and GTILNO values were fixed at 1.3.

3. Results and discussion

We calculated the cross-sections of activation products induced by ^{nat}Cr(d, x)$^{52g,m+}$Mn, ^{nat}Cr(d, x)^{54}Mn, ^{nat}Cr(d, x)^{51}Cr and ^{nat}Cr(d, x)^{48}V for each of the reactions using a default model and another three different level-density models LEVDEN = 1, 2, and 3. We approached the cross-section changes with different value of LEVDEN. The results achieved by EMPIRE were calculated, compared, and evaluated with other literature data sets and data taken from various versions of the online electronic TENDL library 2010 [19], 2012 [20], 2013 [21], 2014 [22], 2015 [23], 2017 [24] and 2019 [25], as shown in Figs. 1 - 4.

3.1. ^{nat}Cr(d, x)$^{52g,m+}$Mn

The theoretical calculated results for the reaction of ^{nat}Cr(d, x)$^{52g,m+}$Mn were obtained using the EMPIRE code (Fig. 1) with available data from Burgus et al. (1954) [26], Kafalas et al. (1956) [27], Cheng Xiaowu et al. (1966) [28], Cogneau et al. (1966) [29], West et al. (1987) [30], Hermanne et al. (2011) [31], Alherbi, (2016) [32], Šimečková et al. (2018) [33] and Bianchi et al. (2020) [17]. The calculation was done using all four level-density models for ^{nat}Cr(d, x)$^{52g,m+}$Mn nuclear reaction.

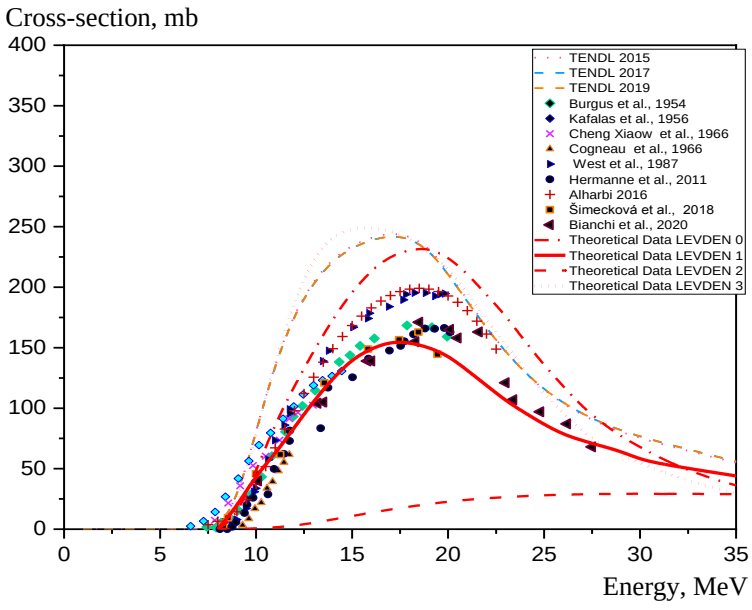

Fig. 1. Theoretical cross-section for ^{nat}Cr(d, x)$^{52g,m+}$Mn by different nuclear level density models using EMPIRE 3.2.2 code. (See color Figure on the journal website.)

As shown in Fig. 1, the cross-section changed with each level-density model. In our experimental-group excitation-function data [17], we were able to calculate the contribution of the cross-section corresponding with the total decay of isomers in relation to the cumulative output of ^{52g}Mn [34]. Therefore, in this nuclear reaction, we also considered the theoretical data as experimental for the calculation of $^{52g,m+}$Mn.

It should be noted that our obtained EMPIRE results have a very good agreement, and the shape of the curve matched all the experimental data sets and TENDL. In the case where we select LEVDEN = 1, we clearly saw that other LEVDEN were significantly different from the experimental data sets. For LEVDEN = 0 the calculated results shown did not match but were higher than all experimental data sets. The LEVDEN = 2 model results predicted a much lower values compared to the results obtained in the experimental cross-section. The LEVDEN = 3 results had good agreement with TENDL-2015, TENDL-2017, and TENDL-2019, and the curve was higher than in the other data sets.

3.2. ^{nat}Cr(d, x)^{54}Mn

The theoretical EMPIRE 3.2.2 code results for the reaction ^{nat}Cr(d, x)^{54}Mn are shown in Fig. 2. In EMPIRE code, the data are clearly showing disagreement with each other, due to different level densities parameterization. The obtained results with the LEVDEN = 1 illustrate a good agreement with the literature and TENDL data sets. However, LEVDEN = 0 in the deuteron energy range 5 - 20 MeV shows a different shape of the curve; LEVDEN = 3 is giving good fitting only with data of Kafalas et al. (1956) [27], LEVDEN = 2 produces higher values in comparison with experimental data at above 20 MeV energies.

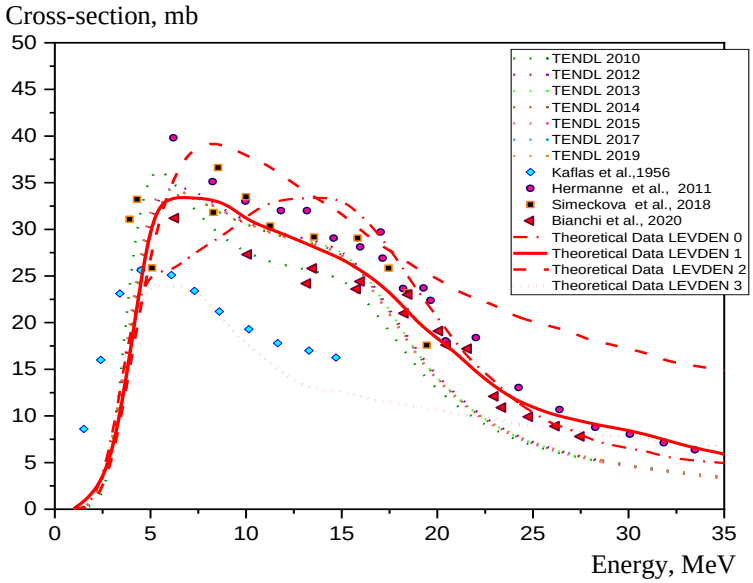

Fig. 2. Theoretical cross-section for ^{nat}Cr(d, x)^{54}Mn by different nuclear level density models using EMPIRE 3.2.2 code. (See color Figure on the journal website.)

3.3. ^{nat}Cr(d, x)^{51}Cr

The theoretical calculations of the ^{nat}Cr(d, x)^{51}Cr for deuteron energy up to 35 MeV are shown in Fig. 3. The EMPIRE code results show that all level densities LEVDEN = 0, 1, and 3 are close to each other demonstrating good accordance with all experimental data. Furthermore, the results of LEVDEN = 1 show a perfect agreement with the results of Coetzee et al. (1972) up to 5.57 MeV [35], and as well as with both Klien et al. (2000) data sets giving good agreement up to 13.34 MeV [36]. In addition, in LEVDEN = 2 model the cross-section values do not reproduce the experimental data above 15 MeV and also the shape of the excitation curve has a dissimilar shape compared with other experimental and TENDL data sets.

3.4. ^{nat}Cr(d, x)^{48}V

The theoretical calculations of the ^{nat}Cr(d, x)^{48}V reaction are shown in Fig. 4. The obtained results predicted by LEVDEN = 1 model are in accordance with all experimental and TENDL data sets. Moreover, the experimental data by Baron et al. (1963) [37] at energy 18.7 MeV show a good agreement with our results obtained with the GSM level-density model. The outcomes with LEVDEN = 0 and LEVDEN = 3 models are very close only at energies less than 25 MeV. Obtained results with LEVDEN = 2 model have shown an extremely high cross-section in respect to the experimental ones, the property of this level density model is due to the non-consideration of misshaping.

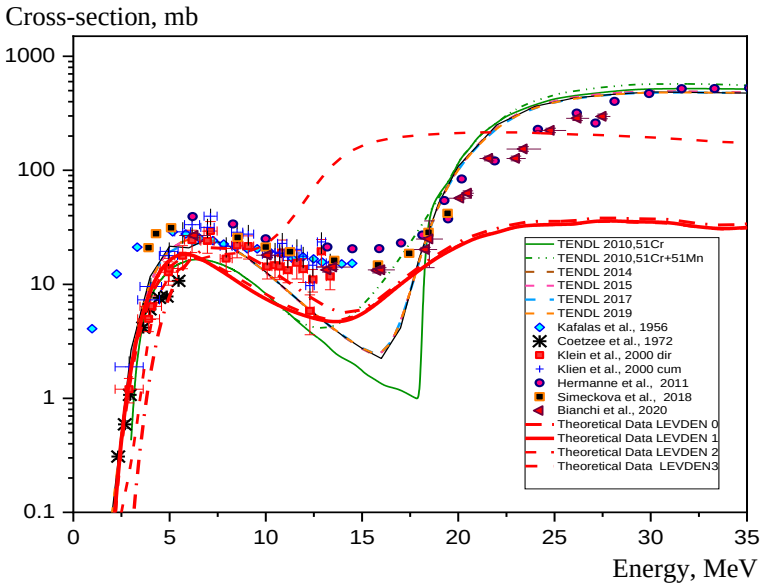

Fig. 3. Theoretical cross-section for $^{nat}Cr(d, x)^{51}Cr$ by different nuclear level density models using EMPIRE 3.2.2 code. (See color Figure on the journal website.)

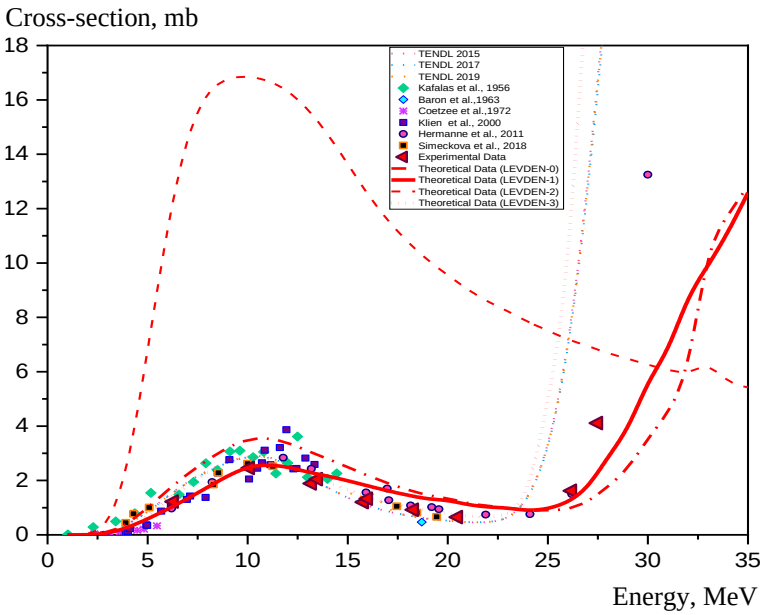

Fig. 4. Theoretical cross-section for $^{nat}Cr(d, x)^{48}V$ by different nuclear level density models using EMPIRE 3.2.2 code. (See color Figure on the journal website.)

4. Conclusions

In this study, calculated theoretical cross-sections of $^{nat}Cr(d, x)^{52g,m+}Mn$, $^{nat}Cr(d, x)^{54}Mn$, $^{nat}Cr(d, x)^{51}Cr$ and $^{nat}Cr(d, x)^{48}V$ reactions were studied using the EMPIRE 3.2.2 computer code with various nuclear level-density models. In EMPIRE code, it is obtained that for all reactions $^{nat}Cr(d, x)^{52g,m+}Mn$, $^{nat}Cr(d, x)^{54}Mn$, $^{nat}Cr(d, x)^{51}Cr$ and $^{nat}Cr(d, x)^{48}V$, the estimated cross-section with parameter LEVDEN = 1 illustrated a good agreement with experimental data. Therefore, LEVDEN = 1 is the best option for the estimation and calculation.

The cross-sections data with LEVDEN = 2 did not show a radical agreement to that found in literature and experimental data. In addition, the predicted cross-section data for LEVDEN = 0 and LEVDEN = 3 is found suitable only for the small, limited range of energy. These calculation results can be advantageous to develop the theoretical models, based on important phenomenological parameters.

We adjusted the input default parameter data for EMPIRE code for each of nuclear reactions $^{nat}Cr(d, x)^{52g,m+}Mn$, $^{nat}Cr(d, x)^{54}Mn$, $^{nat}Cr(d, x)^{51}Cr$, and $^{nat}Cr(d, x)^{48}V$, in order to achieve good agreement with the experimental data. We can conclude that our theoretical calculations are better than those given by the TALYS code. As a result, the theoretical predictions are very close to experimental data. For this reason, the theoretical description is recommended in cases when experimental measurements are difficult to perform.

The work was performed in the cooperation framework of the research Salahaddin University-Erbil and project METRICS by INFN (Italian National Institute of Nuclear Physics, CSN5). The cyclotron ARRONAX is supported by the European Union.

REFERENCES

1. N. Ramamoorthy. Impact of nuclear medicine and radiopharmaceuticals on health-care delivery: Advances, lessons, and need for an objective value-matrix. Indian Journal of Nuclear Medicine 33(4) (2018) 273.
2. Beneficial Use and Production of Isotopes. 2000 Update (Nuclear Energy Agency, OECD, 2000) 82 p.
3. L. Jødal, C. Le Loirec, C. Champion. Positron range in PET imaging: non-conventional isotopes. Physics in Medicine & Biology 59(23) (2014) 7419.
4. P. Martini. High-Yield Cyclotron Production of Metallic Radioisotopes for Nuclear Medicine. Ph.D. Thesis (Italy, Università degli Studi di Ferrara, 2017).
5. S. Jadiyappa. Radioisotope: Applications, Effects, and Occupational Protection. In: Principles and Applications in Nuclear Engineering - Radiation Effects, Thermal Hydraulics, Radionuclide Migration in the Environment, 2018.
6. M.A. Synowiecki, L.R. Perk, J.F.W. Nijsen. Production of novel diagnostic radionuclides in small medical cyclotrons. EJNMMI Radiopharmacy and Chemistry 3 (2018) art. 3.
7. G. Saar et al. Anatomy, functionality, and neuronal connectivity with manganese radiotracers for positron emission tomography. Molecular Imaging and Biology 20(4) 2018 562.
8. M. Herman et al. EMPIRE: nuclear reaction model code system for data evaluation. Nuclear Data Sheets 108(12) (2007) 2655.
9. H. An, C. Cai. Global deuteron optical model potential for the energy range up to 183 MeV. Phys. Rev. C 73(5) (2006) 054605.
10. M. Şekerci, H. Özdoğan, A. Kaplan. Investigation on the Different Production Routes of Ga-67 Radioisotope by Using Different Level Density Models. Moscow University Physics Bulletin 74(3) (2019) 277.
11. M. Şekerci, H. Özdoğan, A. Kaplan. An investigation of effects of level density models and gamma ray strength functions on cross-section calculations for the production of ^{90}Y, ^{153}Sm, ^{169}Er, ^{177}Lu and ^{186}Re therapeutic radioisotopes via (n, γ) reactions. Radiochimica Acta 108(1) (2020) 11.
12. H. Özdoğan, M. Şekerci, A. Kaplan. Investigation of gamma strength functions and level density models effects on photon induced reaction cross-section calculations for the fusion structural materials ^{46,50}Ti, ^{51}V, ^{58}Ni and ^{63}Cu. Applied Radiation and Isotopes 143 (2019) 6.
13. M. Şekerci, H. Özdoğan, A. Kaplan. Level density model effects on the production cross-section calculations of some medical isotopes via (α, xn) reactions where x = 1 - 3. Modern Physics Letters A 35(24) (2020) 2050202.
14. H. Özdoğan, M. Şekerci, A. Kaplan. An Investigation on the Effects of Some Theoretical Models in the Cross-Section Calculations of ^{50,52,53,54}Cr (α, x) Reactions. Phys. Atom. Nucl. 83(6) (2020) 820.
15. H. Özdoğan et al. Estimations of level density parameters by using artificial neural network for phenomenological level density models. Applied Radiation and Isotopes 169 (2021) 109583.
16. M. Herman et al. EMPIRE-3.2 Malta modular system for nuclear reaction calculations and nuclear data evaluation. User's Manual. INDC(NDS)-0603, BNL-101378-2013 (Brookhaven National Laboratory, National Nuclear Data Center, 2013) 297 p.
17. F. Bianchi et al. On the production of ^{52g}Mn by deuteron irradiation on natural chromium and its radionuclidic purity. Applied Radiation and Isotopes 166 (2020) 109329.
18. A. D'Arrigo et al. Semi-empirical determination of the shell correction temperature and spin dependence by means of nuclear fission. Journal of Physics G: Nuclear and Particle Physics 20(2) (1994) 365.
19. https://www-nds.iaea.org/public/download-endf/TENDL-2010/
20. https://www-nds.iaea.org/public/download-endf/TENDL-2012/; J. Koning, D. Rochman. Modern Nuclear Data Evaluation with the TALYS Code System. Nuclear Data Sheets 113(12) (2012) 2841.
21. https://www-nds.iaea.org/public/download-endf/TENDL-2013/
22. https://www-nds.iaea.org/public/download-endf/TENDL-2014/
23. https://tendl.web.psi.ch/tendl_2015/tendl2015.html
24. https://tendl.web.psi.ch/tendl_2017/reference.html; https://www-nds.iaea.org/public/download-endf/TENDL-2017/.
25. https://tendl.web.psi.ch/tendl_2019/talys.html; https://www-nds.iaea.org/public/download-endf/TENDL-2019; J. Koning et al. TENDL: Complete Nuclear Data Library for Innovative Nuclear Science and Technology. Nuclear Data Sheets 155 (2019) 1.
26. W.H. Burgus et al. Cross Sections for the Reactions Ti^{48}(d, 2n)V^{48}; Cr^{52}(d, 2n)Mn^{52}; and Fe^{56}(d, 2n)Co^{56}. Phys. Rev. 95(3) (1954) 750.
27. P. Kafalas, J.W. Irvine Jr. Nuclear excitation functions and thick target yields: (Cr + d). Phys. Rev. 104(3) (1956) 703.
28. C. Xiaowu et al. Some measurements of deuteron induced excitation function at 13 MeV. Acta Physica Sinica 22 (1966) 250.
29. M. Cogneau, L. Gilly, J. Cara. Absolute cross sections and excitation functions for deuteron-induced reactions on chromium between 2 and 12 MeV. Nuclear Physics A 99(1) (1967) 686.
30. H.I. West Jr, R.G. Lanier, M.G. Mustafa. Cr^{52}(p, n)^{52}Mn^{g,m} and Cr^{52}(d, 2n)^{52}Mn^{g,m} excitation functions. Phys. Rev. C 35(6) (1987) 2067.
31. A. Hermanne et al. Cross sections of deuteron induced reactions on ^{nat}Cr up to 50 MeV: Experiments and comparison with theoretical codes. Nucl. Instr. Meth. B 269(21) (2011) 2563.
32. A.A. Alharbi. Experimental Results Evaluation and Theoretical Study for the Production of the Radio Isotope ^{52}Mn Using P, D and A-Projectiles on V and Cr Targets. Arab Journal of Nuclear Sciences and Applications 49(3) (2016) 216.

33. E. Šimečková et a. Consistent account of deuteron-induced reactions on ^{nat}Cr up to 60 MeV. Phys. Rev. C 98(3) (2018) 034606.
34. R.B. Firestone, C.M. Baglin, S.Y. Frank Chu. *Table of Isotopes: 1999 Update.* 8th Edition. 224 p.
35. P.P. Coetzee, M.A. Peisach. Activation cross sections for deuteron-induced reactions on some elements of the first transition series, up to 5.5 MeV. Radiochimica Acta 17(1) (1972) 1.
36. A.T.J. Klein, F. Rösch, S.M. Qaim. Investigation of ^{50}Cr(d, n)^{51}Mn and ^{nat}Cr(p, x)^{51}Mn processes with respect to the production of the positron emitter ^{51}Mn. Radiochimica Acta 88(5) (2000) 253.
37. N. Baron, B.L. Cohen. Activation cross-section survey of deuteron-induced reactions. Phys. Rev. 129(6) (1963) 2636.

Глара Фуад Хасан[1,2,3,*], Едріс Мухаммад-Тахір Нурі[1], Флавія Гроппі[2,3]

[1] Фізичний факультет, Педагогічний коледж, Університет Салахаддіна, Ербіль, Ірак
[2] Фізичний факультет, Міланський університет, Мілан, Італія
[3] Лабораторія прискорювачів та прикладної надпровідності (*LASA*),
Фізичний факультет, Міланський університет і Національний інститут ядерної фізики (*INFN*),
Сеграте, Італія

*Відповідальний автор: gelara.hassan@su.edu.krd

ОЦІНКА ПЕРЕРІЗІВ ДЛЯ РАДІОНУКЛІДІВ, ЩО ВИКОРИСТОВУЮТЬСЯ В ПОЗИТРОННО-ЕМІСІЙНІЙ ТОМОГРАФІЇ, З ВИКОРИСТАННЯМ КОДУ EMPIRE 3.2.2 З РІЗНИМИ МОДЕЛЯМИ ЩІЛЬНОСТЕЙ ЯДЕРНИХ РІВНІВ

Представлено результати розрахунків поперечних перерізів для ядерних реакцій на природному хромі (^{nat}Cr) для деяких радіонуклідів, що використовуються в позитронно-емісійній томографії: ^{nat}Cr(d, x)$^{52g, m+}$Mn, ^{nat}Cr(d, x)^{54}Mn, ^{nat}Cr(d, x)^{51}Cr та ^{nat}Cr(d, x)^{48}V з використанням статистичної ядерної програми EMPIRE 3.2.2 з різними моделями щільності ядерних рівнів. Результати порівняно з експериментальними даними, знайденими в літературі, і даними з різних електронних бібліотек TENDL.

Ключові слова: радіоізотопи Mn, позитронно-емісійна томографія, поперечні перерізи реакцій, ядерна медицина, код EMPIRE 3.2.2.

Надійшла/Received 07.10.2021